

Unveiling *meta*-Alkyloxy/-Silyloxy-Substituted *N*-Aryl PNP Ligands for Efficient Cr-Catalyzed Ethylene Tetramerization

Samir Barman,* Nestor Garcia, E. A. Jaseer,* Mohamed Elanany, Motaz Khawaji, Hassan Alasiri, Abdul Malik P. Peedikakkal, Muhammad Naseem Akhtar, and Rajesh Theravalappil



Cite This: *ACS Omega* 2023, 8, 26437–26443



Read Online

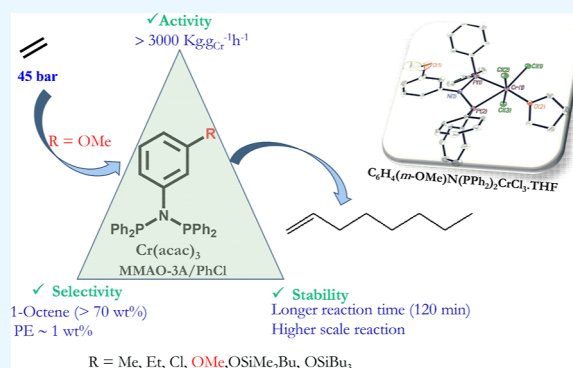
ACCESS |

Metrics & More

Article Recommendations

Supporting Information

ABSTRACT: Novel *N*-aryl-functionalized PNP ligands (1–4) bearing *m*-alkyloxy/-silyloxy substituents were prepared and evaluated for chromium-catalyzed ethylene oligomerization using MMAO-3A as an activator. The selected Cr/PNP system under optimized condition exhibited high 1-octene-selective (up to 70 wt %) ethylene tetramerization at a remarkable rate (over 3000 kg gCr⁻¹ h⁻¹). More importantly, the undesirable polyethylene selectivity was restricted to a minimum level of ~1–2 wt % for pre-catalysts derived with ligands 1 and 2. Employing chlorobenzene as a reaction medium yielded best productivity in conjunction to the total α -olefin (1-C₆ + 1-C₈) selectivity (~88 wt %). *N*-aryl PNP ligands (3 and 4) incorporating *m*-silyloxy substituents in the phenyl ring exhibited relatively poorer tetramerization performance while yielding higher PE fraction as compared to their *m*-alkyloxy derivatives. A detailed molecular structure of the best-performing pre-catalyst 1-Cr was established by single-crystal X-ray diffraction analysis. The stability of 1/Cr-based catalyst system was investigated for a reaction time of up to 2 h under optimized condition.



1. INTRODUCTION

Linear alpha olefins (LAOs) containing 6- and 8-carbon atoms serve as immensely valuable feed stocks for the large-scale production of co-polymers, linear low-density polyethylene (LLDPE) exhibiting outstanding material properties.^{1–10} Industrially, LAOs are manufactured by two main routes: oligomerization of ethylene and by Fischer–Tropsch synthesis followed by purification.⁵ Over the past decade, the catalytic approach to promote selective tri-/tetramerization to access 1-C₆/1-C₈ olefins emerged as a topic of great academic/industrial research interest, thanks to the breakthrough report by the Sasol technology.¹¹ Chromium catalysts incorporating phosphine-based ligands were found to achieve outstanding selective ethylene oligomerization performance.^{6,8,11–18} The bisphosphineamine ligands generally termed as PNPs captivated particular attention owing to their ability to promote ethylene tetramerization to selectively produce 1-octene product.^{8,11–14} In fact, the later class of ligand possessing a great variety of *N*-alkyl, -cycloalkyl and -aryl functionality have been developed and thoroughly investigated. It is evidenced that the electronic as well as the steric profile of the *N*-substituents could play a pivotal role to determine the catalyst efficiency.¹⁴ Recently, we also demonstrate that by introducing a *N*-tritycene moiety, the total alpha selectivity could be increased to an outstanding level (>95 wt %).¹⁹ Here, we strive to develop Cr-based ethylene tetramerization catalysts where various meta-substituted *N*-aryl-functionalized

PNP ligands have been targeted considering that the presence of a suitable substitution at this position of the *N*-phenyl ring could be advantageous to attain higher productivity.^{20,21} We recently demonstrated that the presence of a –CF₃ functional group at the meta position of the *N*-phenyl moiety was able to promote ethylene tetramerization with high efficiency while exhibiting remarkable temperature tolerance ability.²¹ Here, we present four novel *N*-aryl-functionalized PNP ligands C₆H₄(*m*-OMe)N(PPh₂)₂ (1), [N(PPh₂)₂C₆H₄(*m*-OCH₂CH₂)₂CH₂ (2), C₆H₄(*m*-OSiMe₂^tBu)N(PPh₂)₂ (3), and C₆H₄(*m*-OSiⁿBu₃)N(PPh₂)₂ (4) having an alkyloxy (1 and 2) or silyloxy (3 and 4) substituents at the *m*-position of the *N*-phenyl moiety (Figure 1) and their detail ethylene tetramerization performance.

2. EXPERIMENTAL SECTION

2.1. General Comments. All manipulations were performed under an inert atmosphere of dry argon using standard Schlenk techniques. Solvents, aniline precursors, 3-methoxyaniline, 4-methoxyaniline, tert-butyl dimethylsilyl

Received: May 3, 2023

Accepted: July 5, 2023

Published: July 14, 2023



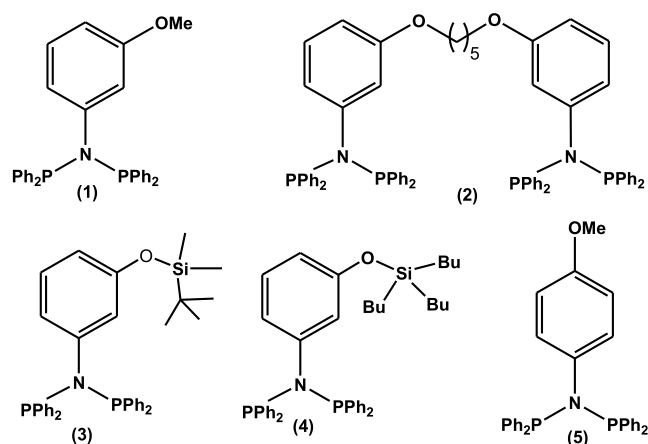
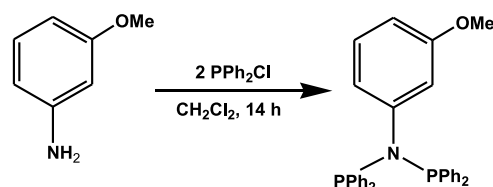


Figure 1. *meta*-Alkyloxy/-silyloxy-substituted *N*-aryl-functionalized PNP ligands evaluated for Cr-catalyzed ethylene tetramerization.

chloride, chlorotributylsilane, 3,3'-(pentamethylenedioxy)-dianiline, Ph_2PCL , Et_3N , and other starting materials including $\text{CrCl}_3 \cdot 3\text{THF}$ were purchased from Sigma-Aldrich. MMAO-3A {modified methylaluminumoxane $[(\text{CH}_3)_{0.7}(\text{iso-C}_4\text{H}_9)_{0.3}\text{AlO}]_n$ 7 wt % solution in *n*-heptane} was purchased from Akzonobel. $\text{Cr}(\text{acac})_3$ (97% purity) was purchased from Strem chemicals. The ethylene gas (99.995% purity) was procured from Abdulla Hashim Gas Co., Saudi Arabia. Solvents and amines were dried using the appropriate reagents and distilled under an argon atmosphere prior to use. The PNP ligand (*i*Pr) $\text{N}(\text{PPh}_2)_2$ was prepared according to the literature procedure.¹¹ The nuclear magnetic resonance (NMR) spectra were obtained at RT using a Bruker 400 MHz instrument. SiMe_4 (for ^1H and ^{13}C) and 85% H_3PO_4 for ^{31}P were used as external standard (GC/FID analyses Agilent Technologies 7890A). Column: PorabOND, 60 m \times 320 μm \times 0.5 μm . The infrared (ATR-IR) spectroscopy was carried out by means of a Thermo Scientific Nicolet iS10 spectrometer in the region of 600–4000 cm^{-1} . The molecular mass of the PNP ligands 1, 3, and 4 was identified using gas chromatography coupled with tandem mass spectrometry (GC–MS/MS) (TQ 8030 Shimadzu). A Rxi-1 MS capillary column (30 m \times id 0.25 mm \times fd 0.25 μm) (Restek, USA) was used for the separation. High-purity helium (99.999%) was employed as a carrier gas at a flow rate of 1.5 mL/min. The sample injection volume was 1.0 μL , and the injector temperature was kept at 300 $^\circ\text{C}$.

2.2. Ligand Preparation. **2.2.1.** $\text{C}_6\text{H}_4(m\text{-OMe})\text{N}(\text{PPh}_2)_2$ (1). To a solution of $\text{C}_6\text{H}_4(m\text{-OMe})\text{NH}_2$ (0.14 g, 1.13 mmol) and triethylamine (0.34 g, 3.40 mmol) in 5 mL of dichloromethane, Ph_2PCL (0.50 g, 2.27 mmol) was slowly added at 0 $^\circ\text{C}$. The mixture was stirred for 1 h and then allowed to warm up to rt and stirring continued for additional 14 h. The volatiles were removed under reduced pressure, and the residue was extracted with anhydrous THF (3 \times 2 mL). The solvent was then removed, and the remaining solid residue was triturated with anhydrous CH_3CN (5 \times 3 mL). The final compound was dried under vacuum to give ligand 1 (Scheme 1) in 59% yield. ^1H NMR (CDCl_3): δ 3.34 (s, 3H, $-\text{OCH}_3$), 6.12 (s, 1H, Ar), 6.35 (d, 1H, Ar), 6.58 (d, 1H, Ar), 6.89 (t, 1H, Ar), 7.25–7.43 (m, 20H, Ar) ppm; ^{13}C NMR (CDCl_3): 55.31, 112.12, 114.39, 121.92, 129.07, 129.36, 133.49, 139.53, 148.84, 159.39; ^{31}P NMR: δ 66.78 (s) ppm. ATR-IR: 3073, 3055, 3000, 2958, 2929, 2831, 1593, 1574, 1477, 1432, 1308, 1283, 1252, 1187, 1168, 1145, 1092, 1048, 998, 962, 948, 901, 872,

Scheme 1. Synthetic Scheme for the Preparation of *m*-OMe-Substituted PNP Ligand 1

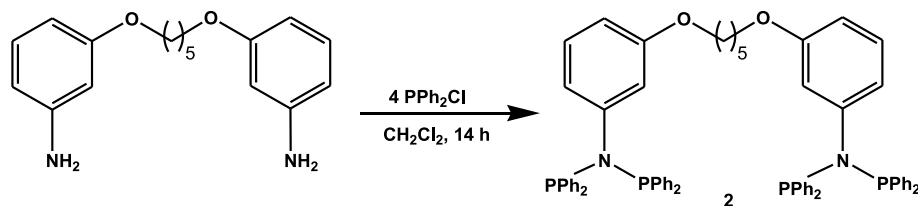
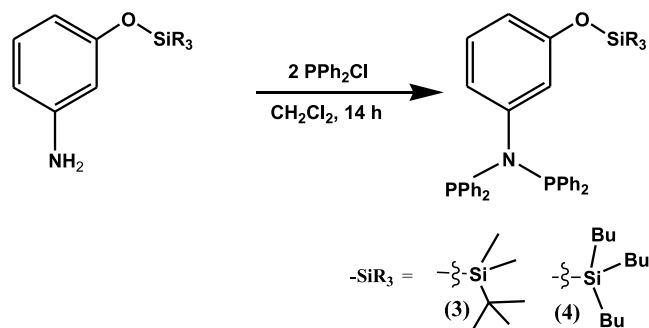


849, 787, 772, 749, 740, 693 cm^{-1} . GC–MS: m/z (491). Elemental microanalysis: Calculated (%) for $\text{C}_{31}\text{H}_{27}\text{NOP}_2$, H 5.54, C 75.75, N 2.85; found, (%) H 5.18, C 75.44, N 2.71.

2.2.2. $[\text{Cr}\{(\text{C}_6\text{H}_4(m\text{-OMe})\text{N}(\text{PPh}_2)_2)\}_2\text{Cl}_3(\text{THF})]$. $\text{C}_6\text{H}_4(m\text{-OMe})\text{N}(\text{PPh}_2)_2$ (0.05 g, 0.10 mmol) and $\text{CrCl}_3(\text{THF})_3$ (0.04 g, 0.10 mmol) were dissolved in dichloromethane (0.7 mL) and stirred for 1 h at room temperature to yield dark green powder material following removal of volatiles (yield 80%). Single crystal was grown from a mixture of dichloromethane and hexane. Elemental microanalysis: calculated (%) for $\text{C}_{35}\text{H}_{35}\text{Cl}_3\text{CrNO}_2\text{P}_2$, H 4.89, C 58.23, N 1.94; found (%), H 4.93, C 58.05, N 2.06. Due to the paramagnetic nature, the NMR spectroscopic analysis of the Cr complex was unsuccessful.

2.2.3. $[\text{N}(\text{PPh}_2)_2\text{C}_6\text{H}_4(m\text{-OCH}_2\text{CH}_2)_2\text{CH}_2$ (2). To a solution of 3,3'-(pentamethylenedioxy)dianiline (0.47 g, 1.63 mmol) and triethylamine (1.0 g, 9.90 mmol) in 8 mL of dichloromethane, Ph_2PCL (1.44 g, 6.57 mmol) was slowly added at 0 $^\circ\text{C}$. The mixture was stirred for 1 h and allowed to warm up to r.t. followed by additional stirring for 14 h. The volatiles were removed under reduced pressure, and the residue was extracted with anhydrous THF (3 \times 4 mL). The solvent was then removed, and the remaining solid residue was triturated with anhydrous CH_3CN (5 \times 3 mL). The final compound was dried under vacuum to give ligand 2 (Scheme 2) as a white solid in 67% yield. ^1H NMR (CDCl_3): δ 1.24–1.85 (m, 6H, $-\text{CH}_2-$), 3.37 (t, 4H, $-\text{OCH}_2-$), 6.08 (s, 2H, Ar), 6.30 (d, 2H, Ar), 6.53 (d, 2H, Ar), 6.86 (t, 2H, Ar), 7.25–7.43 (m, 40H, Ar) ppm; ^{13}C NMR (CDCl_3): 22.69, 28.37, 67.38, 112.57, 114.63, 121.38, 128.15, 129.16, 133.40, 139.49, 148.59, 159.07 ppm; ^{31}P NMR (CD_2Cl_2): δ 66.76 (s) ppm. ATR-IR: 3073, 3049, 2946, 2860, 1596, 1577, 1478, 1433, 1388, 1308, 1285, 1255, 1170, 1150, 1090, 1044, 1027, 1010, 998, 900, 872, 844, 770, 740, 693 cm^{-1} . Elemental microanalysis: calculated (%) for $\text{C}_{65}\text{H}_{58}\text{N}_2\text{O}_2\text{P}_4$, H 5.71, C 76.31, N 2.74; found (%), H 5.82, C 75.94, N 2.79.

2.2.4. $\text{C}_6\text{H}_4(m\text{-OSiMe}_2^t\text{Bu})\text{N}(\text{PPh}_2)_2$ (3). To a solution of $\text{C}_6\text{H}_4(m\text{-OSiMe}_2^t\text{Bu})\text{NH}_2$ ²² (0.37 g, 1.65 mmol) and triethylamine (0.50 g, 4.95 mmol) in 5 mL of dichloromethane, Ph_2PCL (0.72 g, 3.3 mmol) was slowly added at 0 $^\circ\text{C}$. The mixture was stirred for 1 h and allowed to warm up to r.t. followed by additional stirring for 14 h. The volatiles were removed under reduced pressure, and the residue was extracted with anhydrous THF (3 \times 3 mL). The solvent was then removed, and the remaining solid residue was triturated with anhydrous CH_3CN (5 \times 3 mL). The final compound was dried under vacuum to give ligand 3 (Scheme 3) as an off-white solid in 61% yield. ^1H NMR (CD_2Cl_2): δ -0.08 (s, 6H, $-\text{CH}_3$), 0.86 (s, 9H, $-\text{C}(\text{CH}_3)_3$), 6.23 (s, 1H, Ar), 6.28 (d, 1H, Ar), 6.51 (d, 1H, Ar), 6.80 (t, 1H, Ar), 7.25–7.44 (m, 20H, Ar) ppm; ^{13}C NMR (CD_2Cl_2): δ -4.67 , 18.14, 25.4, 111.19, 117.32, 120.52, 128.09, 128.57, 129.14, 131.26, 133.22, 139.30, 148.66, 155.55; ^{31}P NMR (CD_2Cl_2): δ 67.24 (s) ppm.

Scheme 2. Synthetic Scheme for the Preparation of **2**Scheme 3. Synthetic Scheme for the Preparation of *m*-Silyloxy-Substituted *N*-Aryl PNP Ligands **3** and **4**

ATR-IR: 3070, 3049, 2949, 2928, 2856, 1578, 1474, 1433, 1362, 1279, 1257, 1167, 1151, 1090, 1027, 990, 903, 887, 871, 836, 807, 786, 714, 693 cm^{-1} . GC-MS: m/z (591). Elemental microanalysis: calculated (%) for $\text{C}_{36}\text{H}_{39}\text{NOP}_2\text{Si}$, H 6.64, C 73.07, N 2.37; found (%), H 6.72, C 73.34, N 2.29.

2.2.5. $\text{C}_6\text{H}_4(m\text{-OSi}^i\text{Bu}_3)\text{NH}_2$. To a mixture of $\text{C}_6\text{H}_4(m\text{-OSi}^i\text{Bu}_3)\text{NO}_2$ (1.74 g, 5.16 mmol) and Raney nickel (~50 mg) in 5 mL of tetrahydrofuran, hydrazine monohydrate (1.55 mL, 31.96 mmol) was slowly added at room temperature inside the glovebox after which the flask was taken out and allowed to stir for 1 h at boiling temperature. The mixture was cooled, passed through a celite filter pad, and volatiles were removed under reduced pressure to yield the desired amine compound (yield: 1.20 g, 76%). ^1H NMR (CDCl_3): δ 0.62–0.74 (m, 6H, $-\text{CH}_2-$), 0.78–0.91 (m, 6H, $-\text{CH}_2-$), 1.20–1.37 (m, 9H, $-\text{CH}_3$ and m, 6H, $-\text{CH}_2-$), 6.17 (m, 1H, Ar), 6.25 (m, 2H, Ar), 6.96 (t, 1H, Ar) ppm; ^{13}C NMR (CDCl_3): 13.91, 14.89, 25.35, 26.64, 107.19, 108.51, 110.51, 130.02, 147.72, 156.76. Elemental microanalysis: calculated (%) for $\text{C}_{18}\text{H}_{33}\text{NOSi}$, H 10.82, C 70.30, N 4.55; found (%), H 10.77, C 70.14, N 4.39.

2.2.6. $\text{C}_6\text{H}_4(m\text{-OSi}^i\text{Bu}_3)\text{N}(\text{PPh}_2)_2$ (**4**). To a solution of $\text{C}_6\text{H}_4(m\text{-OSi}^i\text{Bu}_3)\text{NH}_2$ (0.507 g, 1.65 mmol) and triethylamine (0.50 g, 4.95 mmol) in 5 mL of dichloromethane, Ph_2PCL (0.72 g, 3.3 mmol) was slowly added at 0 $^\circ\text{C}$. The mixture was stirred for 1 h and allowed to warm up to r.t. followed by additional stirring for 14 h. The volatiles were removed under reduced pressure, and the residue was extracted with anhydrous THF (3×3 mL). An oily compound of **4** was obtained after removing the solvent under vacuum, 59% yield (Scheme 3). ^1H NMR (CD_2Cl_2): δ 0.58–0.75 (m, 6H, $-\text{CH}_2-$), 0.86–0.92 (m, 6H, $-\text{CH}_2-$), 1.18–1.38 (m, 9H, $-\text{CH}_3$ and m, 6H, $-\text{CH}_2-$), 6.24 (s, 1H, Ar) 6.50 (d, 1H, Ar), 6.60 (d, 1H, Ar) 6.79 (t, 1H, Ar) 7.23–7.50 (m, 20H, Ar) ppm; ^{13}C NMR (CD_2Cl_2): 13.48, 13.75, 25.11, 26.50, 110.68, 116.79, 119.69, 121.84, 128.09, 128.57, 129.12, 131.26, 133.23, 139.34, 147.84, 156.72; ^{31}P NMR (CD_2Cl_2): δ 67.09 (s) ppm. ATR-IR: 3067, 3055, 2955, 2921, 2870, 1588, 1479, 1464, 1434, 1376, 1279, 1169, 1150, 1080, 1027, 991, 915, 886, 846,

739, 692 cm^{-1} . GC-MS: m/z (676). Elemental microanalysis: calculated (%) for $\text{C}_{42}\text{H}_{51}\text{NOP}_2\text{Si}$, H 7.61, C 74.63, N 2.07; found (%), H 7.70, C 74.54, N 2.09.

2.3. General Oligomerization Procedure. All runs for ethylene oligomerization were carried out in a 250 mL stainless steel (vessel) Buchi reactor system equipped with a propeller like stirrer (1000 rpm) and injection barrel. Co-catalyst diluted in 98 mL of the desired solvent and pre-catalyst mixture [containing $\text{Cr}(\text{acac})_3$ and **1–4** dissolved in 2 mL of chlorobenzene] was charged to the reactor and pressurized with ethylene at 45 bar at required temperature. The reaction temperature was maintained during the reaction by circulating hot oil in the jacket and by allowing the cool liquid to flow from the chiller through the cooling coil present inside the reactor vessel. SCADA software controlled the reaction temperature and pressure of the reactor precisely using an electronic pressure controller. After the desired reaction time, 2 mL of methanol was injected to quench the reaction which was then cooled and depressurized slowly to atmospheric pressure. The small portion of the crude products was filtered and analyzed using GC-FID. The remaining mixture was added to 50 mL of acidic methanol (5% HCl), and the polymeric products were recovered by filtration, washed three times with distilled water, and dried overnight in a vacuum oven at 60 $^\circ\text{C}$.

3. RESULTS AND DISCUSSION

The treatment of amine precursors 3-methoxyaniline and 3,3'-(pentamethylenedioxy)dianiline with chlorodiphenylphosphine in the presence of triethylamine base resulted off white powder compounds **1** and **2**, respectively, in good yield (see Section 2.2 for detail). The ^1H and ^{13}C NMR spectra of **1** suggest the formation of the targeted ligand (Figure S1, Supporting Information). The aromatic protons appear in the range of 6.12–7.38 ppm while the protons corresponding to the $-\text{OMe}$ group can be seen at 3.34 ppm. The ^{31}P NMR spectrum of **1** (Figure S2, left) displayed an intense peak at 66.78 ppm, which can be attributed to the P-atom of the PNP ligand.¹¹ Similarly, the ^{31}P NMR spectrum of ligand **2** also displayed a phosphorus signal at 66.76 ppm (Figure S2, right), thus affirming the presence of a PNP moiety. The bridged methylene protons adjacent to the phenoxy moiety appear at 3.40 ppm in the ^1H NMR spectrum, while the remaining bridged methylene protons can be seen at 1.56 and 1.34 ppm (Section 2.2). Additionally, the ^{13}C NMR signals of **2** were also found in good agreement with the expected PNP ligand.

To access the silyloxy group containing *N*-aryl PNP ligands **3** and **4**, the amine precursors 3-(tert-butylsilyloxy)aniline and 3-(tributylsilyloxy)aniline, which was prepared by a two-step syntheses procedure starting from 3-nitrophenol,²³ were treated with chlorodiphenylphosphine (Scheme 3 and Section 2.2), respectively, under a similar reaction procedure noted above. As expected, typical ^{31}P signals at 67.24 and 67.09 ppm ascribable to the PNP compounds could be

Table 1. Temperature and Solvent-Dependent Ethylene Tetramerization Study Using the Cr(acac)₃/1/MMAO-3A System^a

entry	solvent	productivity (kg g _{Cr} ⁻¹ h ⁻¹)	product selectivity (wt %)					
			1-C ₆	C ₆ cyclics	1-C ₈	1-C ₆ + 1-C ₈	C ₁₀₊	PE
1	CyH	400	16.0	7.2	69.5	85.5	0.7	0.7
2	MeCy	608	14.6	8.4	68.6	83.1	1.4	0.9
3	DHN	655	15.0	9.0	67.8	82.9	1.1	1.5
4	PhCl	3342	20.8	7.8	67.9	88.7	1.4	1.0
5 ^b	PhCl	1890	16.2	8.7	70.3	86.6	2.0	1.4
6 ^c	PhCl	871	33.4	5.7	57.0	90.4	0.3	1.6

^aConditions: Cr(acac)₃ 1 μmol, MMAO-3A 2 mmol (Al/Cr 2000), L/Cr = 1, total solution volume 100 mL, 60 °C, 45 bar, 10 min. ^b45 °C. ^c75 °C.

Table 2. Cr Source and Ligand Screening for the Ethylene Tetramerization Study^a

entry	ligand	productivity (kg g _{Cr} ⁻¹ h ⁻¹)	product selectivity (wt %)					
			1-C ₆	C ₆ cyclics	1-C ₈	1-C ₆ + 1-C ₈	C ₁₀₊	PE
1	5	2180	22.6	7.6	66.2	88.8	1.5	0.8
2	iPrN(PPh ₂)	680	28.7	3.5	59.7	88.4	1.7	3.1
3 ^b	iPrN(PPh ₂)	1184	18.6	4.2	69.9	88.5	1.6	3.5
4	2	2208	20.7	8.3	66.7	87.4	1.6	1.1
5 ^c	1-Cr	2000	21.1	7.8	67.8	88.9	1.2	0.4
6 ^d	1	1669	21.3	7.6	67.5	88.8	1.1	0.6
7 ^e	1	1500	11.7	9.4	70.3	82.0	5.5	1.6
8 ^f	1	657	11.7	9.4	70.0	82.0	5.5	1.3

^aConditions: Cr(acac)₃ 1 μmol, L/Cr = 1, MMAO-3A 2 mmol (Al/Cr 2000), PhCl, total solution volume 100 mL, 60 °C, 45 bar, 10 min. ^b45 °C. ^c1-Cr = CrCl₃ (THF-OMePNP complex). ^dCrCl₃ 3THF. ^e60 min, 45 °C. ^f120 min, 45 °C [Cr(acac)₃ 2 μmol, L/Cr = 1, MMAO-3A 4 mmol (Al/Cr 2000), total reaction volume 200 mL].

observed for ligand 3 and 4, respectively (Figure S3, Supporting Information). The ¹H and ¹³C chemical shift values were also found in accordance with their expected structure (Section 2.2). The *p*-OMe-substituted *N*-aryl PNP ligand 5 was prepared according to the literature procedure.¹⁴

Tetramerization of ethylene using the chromium catalyst formed with the *m*-OMe-substituted ligand, Cr(acac)₃/1/MMAO-3A, in various solvents (cyclohexane, methylcyclohexane, decahydronaphthalene, and chlorobenzene) at 60 °C was performed. The results presented in Table 1 (entries 1–4) reveal that among all the solvents examined, chlorobenzene performs best in terms of the oligomerization reaction rate, yielding productivity of 3342 kg g_{Cr}⁻¹ h⁻¹ and total α-olefins (1-C₆ + 1-C₈) selectivity (88.7 wt %, entry 4). The octene fraction observed in other solvents (entries 1–3), however, was quite similar (~68–69 wt %). More importantly, the polyethylene (PE) selectivity was controlled within 0.7–1.5 wt %. The reaction at 45 °C in chlorobenzene gave slightly improved octene selectivity (70.3 wt %) at productivity 1890 kg g_{Cr}⁻¹ h⁻¹ (entry 5). At higher temperature (75 °C), both the rate of the reaction as well as the 1-octene selectivity were significantly reduced to 871 kg g_{Cr}⁻¹ h⁻¹ and 57 wt %, respectively (entry 6). These results seemed to indicate a partial catalyst decomposition at higher temperature. A comparative temperature-dependent catalytic performance of the Cr(acac)₃/1/MMAO-3A system in chlorobenzene is presented in Figure S4. We note that when the temperature rises from 45 to 75 °C, 1-hexene selectivity increases from 16.2 to 33.4 wt %, C₆ cyclics reduces from 8.7 to 5.7 wt %, and the C₁₀₊ fraction reduces from 2 to 0.3 wt %. These observations tend to suggest that trimerization is favorable at higher temperature over tetramerization.

For a direct comparison purpose, the *p*-OMe-substituted analogous ligand 5 (earlier reported by Sasol)¹⁴ was also tested

under our optimized condition, which indicates that the shifting of -OMe functionality at the *p*-position of the phenyl ring has minimal effect on C₈ olefin selectivity, however, exerts a significant detrimental effect on the rate of the reaction. Thus, a lower productivity of 2180 kg g_{Cr}⁻¹ h⁻¹ (Table 2, entry 1) could only be achieved. To further comprehend the tetramerization performance of Cr(acac)₃/1/MMAO-3A, a catalytic run using Sasol's benchmark Cr-system Cr(acac)₃/(ⁱPr)N(PPh₂)₂/MMAO-3A was conducted under identical condition. Based on the data in Table 2 (entries 2 and 3), it is apparent that the later system yields significantly lower productivities (680 and 1184 kg g_{Cr}⁻¹ h⁻¹ at 60 and 45 °C, respectively) even though the 1-octene selectivity at lower temperature was somewhat similar (~70 wt %). The PE fraction observed for the benchmark system is also considerably higher (>3 wt %). Next, a catalytic run at 60 °C using bis-*N*-aryl PNP ligand 2 was performed, and data are presented in Table 2 (entry 4). As expected, the Cr(acac)₃/2/MMAO-3A system was also able to promote ethylene tetramerization with high reaction rate 2208 kg g_{Cr}⁻¹ h⁻¹ and excellent selectivity toward 1-octene. More significantly, the PE selectivity was again maintained just about 1 wt %. Nonetheless, the overall catalytic performance exhibited by the 2/Cr system is somewhat weaker in comparison to the ligand 1-based system.

The outstanding catalytic results achieved by ligand 1-supported Cr system further encouraged us to elucidate the molecular structure of the potential pre-catalyst. To obtain high-quality crystalline compound, 1 was reacted with the CrCl₃ 3THF complex followed by crystallization (see Section 2.2 for detail). Note that the Cr(acac)₃ complex used for the catalytic reaction in Table 1 is typically non-reactive to the PNP ligand in the absence of an activator. The single crystal thus obtained was analyzed by the X-ray diffraction study,

which reveals a monomeric 1-CrCl₃(THF) complex with distorted octahedral geometry around the Cr atom (Figure 2).

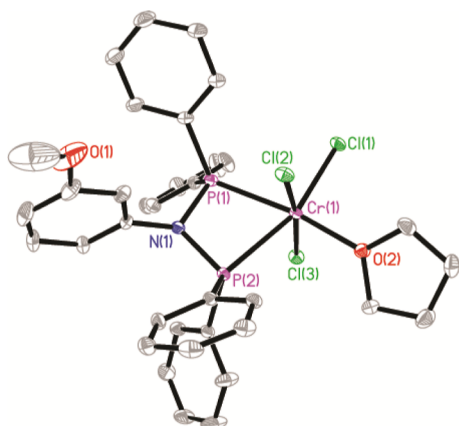


Figure 2. Molecular structure of ligand 1-Cr with 15% probability. H atoms have been omitted for clarity. Selected bond distances and angles: Cr(1)–P(1) 2.4376(14) Å; Cr(1)–P(2) 2.5122(13) Å; P(1)–Cr(1)–P(2) 67.51(4)°; and P(1)–N(1)–P(2) 106.8(2)°.

A similar structural feature was earlier established for the *m*-CF₃-substituted PNP ligand-supported chromium complex.²¹ It is worthy to mention at this point that the preformed L-Cr(III) complexes (L = phosphineamine ligands)^{11,24,25} typically favor dimeric structural features. Nevertheless, few monomeric preformed Cr(III) complexes could also be found in the literature where the Cr metal is found to be coordinated by the PNP- and phospholane-based ligands.²⁶ The P1–Cr–P2 bite angle of 67.51(4)° was seen for 1-Cr, which is slightly higher (vs 65.5°) as compared to that being observed for the benchmark ligand-supported chromium complex, (Pr)₃N-(PPh₂)₂/Cr.²⁶ The Cr–P bond distances of 2.4376(14) and 2.5122(13) Å are observed for 1-Cr while P–N–P angle is estimated to be 106.8(2)°. After establishing the molecular structure of the pre-catalysts 1-Cr, a catalytic run using the same was performed under optimized reaction condition, and the data are presented in entry 5 (Table 2), to our surprise a notable drop in the reaction rate was observed. Thus yielding a productivity of 2000 kg g_{Cr}^{−1} h^{−1}, even though the product selectivity especially toward 1-octene was maintained at 67.8 wt %. Incidentally, a similar reactivity trend was also observed when an *in situ* formed catalyst, generated by injecting 1, CrCl₃(THF) and MMAO-3A separately into the reactor, was employed to carry out the tetramerization reaction (Table 2, entry 6). These results suggest that apart from the effect of PNP ligand 1, the secondary ligands, *i.e.*, chloride (−Cl) and acetylacetonate (*acac*) also could play an important role to

alter the ethylene tetramerization profile, and the *acac* ligand containing metal precursor appeared to be favorable to attain higher reaction rate.

After establishing 1 as a potential ligand, we carried out additional experiments to evaluate its performance for longer reaction time at 45 °C, the temperature where best selectivity toward 1-octene was achieved. Interestingly, the data reveal that (Table 2, entry 7) even after a run time of 1 h, the catalyst system Cr(*acac*)₃/1/MMAO-3A was able to maintain high 1-octene selectivity (>70 wt %) at a reaction rate of 1500 kg g_{Cr}^{−1} h^{−1}. Based on these results, it could be surmised that the catalytic path, involving chromacyclononane intermediate, leading to the 1-octene product remains unaffected to the reaction time parameter. A similar selectivity trend was again maintained for a reaction time of 2 h while increasing the total reaction volume up to 200 mL, even though a drop in productivity was noticed (entry 8). The exact reason for the drop in the reaction rate is not clear however we presume, based on our observation of the ethylene flow during reaction, that the ethylene solubility is likely to be negatively impacted as the product concentration increases into the reaction vessel.

To further extend our study on evaluating the effect of *m*-substituted *N*-aryl PNPs, we performed ethylene tetramerization reactions using *m*-silyloxy-substituted ligands (3 and 4)-supported Cr-system in detail. The results summarized in Table 3 reveal that both the *m*-silyloxy-substituted PNP-supported Cr-catalysts, *i.e.*, Cr(*acac*)₃/3/MMAO-3A and Cr(*acac*)₃/4/MMAO-3A could promote ethylene tetramerization with excellent rate while the best productivity of 2686 kg g_{Cr}^{−1} h^{−1} (entry 2) could be attained for the ligand 3-based system. Moreover, both the catalysts exhibited higher reaction rate at 60 °C, which is in line with the results obtained for the ligand 1-based Cr-catalyst. To the contrary, a significantly higher PE fraction could be observed even though the C10+ product selectivity was maintained below 1.5 wt %. Most notably, ligand 4 possessing a tributylsilyl (TBS) moiety performed worst in terms of PE formation, thereby indicating a detrimental effect of three *n*-butyl substitution on the silicon atom to mitigate the selective oligomerization process while relatively favoring the coordination insertion mechanism leading to the formation of PE byproducts.

Overall, the methoxy substitution at the *meta* position of the *N*-phenyl ring, *i.e.*, ligand 1 is turned out to be the most efficient PNP ligand for Cr-catalyzed ethylene tetramerization. In fact, the reaction rate in conjunction to the 1-octene selectivity achieved by this ligand-based Cr-system is much superior as compared to those with ligand 2 and other PNPs having a *m*-silyloxy (*i.e.*, ligand 3 and 4), −Me, −Et, and −Cl groups²¹ (Table 4, Figures S5–S9). Most significantly, the ligand 1-based Cr-catalyst is also able to restrict the PE fraction

Table 3. Ethylene Tetramerization Using the Cr(*acac*)₃/*m*-OSiR–C₆H₄–N(PPh₂)₂/MMAO-3A System^a

entry	ligand	temperature (°C)	productivity (kg g _{Cr} ^{−1} h ^{−1})	product selectivity (wt %)					
				1-C ₆	C ₆ cyclics	1-C ₈	1-C ₆ + 1-C ₈	C ₁₀₊	PE
1	3	45	1485	14.5	8.0	68.7	83.2	2.2	3.2
2	3	60	2686	24.0	6.3	63.5	87.5	1.3	3.5
3	3	75	1171	29.7	5.2	56.5	86.2	0.3	6.3
4	4	45	1209	13.2	7.7	69.3	82.5	2	4.6
5	4	60	2036	19.0	6.6	62.2	81.1	0.9	9.6
6	4	75	894	27.6	5.0	51.7	79.3	0.1	13.3

^aConditions: Cr(*acac*)₃ 1 μmol, MMAO-3A 2 mmol (Al/Cr 2000), L/Cr = 1, total solution volume 100 mL, PhCl, 45 bar, 10 min.

Table 4. Ethylene Tetramerization Performance Comparison Using Cr-Catalysts Supported by Various PNP Ligands at 60 °C^a

entry	ligand	productivity (kg g _{Cr} ⁻¹ h ⁻¹)	product selectivity(wt %)			
			1-C ₆	1-C ₈	1-C ₆ + 1-C ₈	PE
1	<i>m</i> -OMe-Ar-PNP (1)	3342	20.8	67.9	88.7	1.0
2	O(CH ₂) ₅ O-(ArPNP) ₂ (2)	2208	20.7	66.7	87.4	1.1
3	<i>m</i> -OTBDMS-C ₆ H ₄ -N(PPh ₂) ₂ (3)	2686	24	63.5	87.5	3.5
4	<i>m</i> -OTBS-C ₆ H ₄ -N(PPh ₂) ₂ (4)	2036	19	62.2	81.1	9.6
5	<i>m</i> -Me-Ar-PNP	1623	21.1	67.7	88.8	1.0
6	<i>m</i> -Et-Ar-PNP	1730	19.7	67.8	87.5	1.3
7	<i>m</i> -Cl-Ar-PNP	2219	20.2	67.8	88.6	1.2

^aConditions: Cr(acac)₃ 1 μmol, MMAO-3A 2 mmol (Al/Cr 2000), L/Cr = 1, total solution volume 100 mL, PhCl, 45 bar, 10 min.

within 1 wt % under the best-performing reaction condition (Table 4 and Figure S9).

4. CONCLUSIONS

Novel *N*-aryl PNP ligands bearing alkyloxy/silyloxy substitution at the *meta* position of the *N*-phenyl ring have been developed and thoroughly investigated toward the Cr-catalyzed selective ethylene tetramerization reaction. Based on detailed catalytic studies, we demonstrate the fact that apart from the reaction medium and metal source, the presence of a suitable functional group at a specific position could play a critical role to accomplish the outstanding reaction rate and 1-octene selectivity. Indeed, the Cr-catalyst formed with the *m*-OMe-substituted *N*-aryl PNP ligand could exhibit remarkable ethylene tetramerization activity. Given its ability to maintain overall ethylene tetramerization performance coupled with minimum PE formation for an extended period of time, the ligand 1-based Cr-catalyst can be envisaged to be a potential candidate for on-purpose 1-C₈ production application.

ASSOCIATED CONTENT

Supporting Information

The Supporting Information is available free of charge at <https://pubs.acs.org/doi/10.1021/acsomega.3c03029>.

NMR spectra, crystallographic details, and catalytic study (PDF)

Crystallographic data for 1-Cr (PDF)

Crystallographic data for AMOMePNPCr (CIF)

AUTHOR INFORMATION

Corresponding Authors

Samir Barman – Center for Refining and Advanced Chemicals, King Fahd University of Petroleum and Minerals, Dhahran 31261, Saudi Arabia; Email: samir.barman@kfupm.edu.sa

E. A. Jaseer – Center for Refining and Advanced Chemicals, King Fahd University of Petroleum and Minerals, Dhahran 31261, Saudi Arabia; orcid.org/0000-0002-5385-8778; Email: jaseer@kfupm.edu.sa

Authors

Nestor Garcia – Center for Refining and Advanced Chemicals, King Fahd University of Petroleum and Minerals, Dhahran 31261, Saudi Arabia

Mohamed Elanany – Fuels and Chemicals Division Aramco Research Center at KAUST, Thuwal 23955, Saudi Arabia

Motaz Khawaji – Fuels and Chemicals Division Aramco

Research Center at KAUST, Thuwal 23955, Saudi Arabia

Hassan Alasiri – Center for Refining and Advanced Chemicals, King Fahd University of Petroleum and Minerals, Dhahran

31261, Saudi Arabia; Chemical Engineering Department, King Fahd University of Petroleum and Minerals, Dhahran 31261, Saudi Arabia; orcid.org/0000-0003-4043-5677

Abdul Malik P. Peedikakkal – Department of Chemistry and Interdisciplinary Research Center for Hydrogen and Energy Storage, King Fahd University of Petroleum and Minerals, Dhahran 31261, Saudi Arabia; orcid.org/0000-0002-4745-2843

Muhammad Naseem Akhtar – Center for Refining and Advanced Chemicals, King Fahd University of Petroleum and Minerals, Dhahran 31261, Saudi Arabia; orcid.org/0000-0001-9884-3935

Rajesh Theravalappil – Center for Refining and Advanced Chemicals, King Fahd University of Petroleum and Minerals, Dhahran 31261, Saudi Arabia

Complete contact information is available at:

<https://pubs.acs.org/10.1021/acsomega.3c03029>

Notes

The authors declare no competing financial interest.

ACKNOWLEDGMENTS

The authors acknowledge the support provided by the Saudi Aramco for funding the project # CRP02285. The support of King Fahd University of Petroleum & Minerals (KFUPM), Dhahran, Saudi Arabia is highly appreciated.

REFERENCES

- (1) Carter, A.; Cohen, S. A.; Cooley, N. A.; Murphy, A.; Scutt, J.; Wass, D. F. High activity ethylene trimerisation catalysts based on diphosphine ligands. *Chem. Commun.* **2002**, 858–859.
- (2) Dixon, J. T.; Green, M. J.; Hess, F. M.; Morgan, D. H. Advances in selective ethylene trimerisation—a critical overview. *J. Organomet. Chem.* **2004**, 689, 3641–3668.
- (3) McGuinness, D. S. Olefin Oligomerization via Metallocycles: Dimerization, Trimerization, Tetramerization, and Beyond. *Chem. Rev.* **2011**, 111, 2321–2341.
- (4) Agapie, T. Selective ethylene oligomerization: Recent advances in chromium catalysis and mechanistic investigations. *Coord. Chem. Rev.* **2011**, 255, 861–880.
- (5) van Leeuwen, P. W. N. M.; Clément, N. D.; Tschan, M. J. L. New processes for the selective production of 1-octene. *Coord. Chem. Rev.* **2011**, 255, 1499–1517.
- (6) Belov, G. P. Tetramerization of ethylene to octene-1 (a review). *Pet. Chem.* **2012**, 52, 139–154.
- (7) Breuil, P.-A. R.; Magna, L.; Olivier-Bourbigou, H. *Catal. Lett.* **2015**, 145, 173–192.
- (8) Alferov, K. A.; Belov, G. P.; Meng, Y. Chromium catalysts for selective ethylene oligomerization to 1-hexene and 1-octene: Recent results. *Appl. Catal., A* **2017**, 542, 71–124.

- (9) Bariashir, C.; Huang, C.; Solan, G. A.; Sun, W. H. Recent advances in homogeneous chromium catalyst design for ethylene tri- and tetramerization. *Coord. Chem. Rev.* **2019**, *385*, 208–229.
- (10) Hao, B.-B.; Alam, F.; Jiang, Y.; Wang, L.; Fan, H.; Ma, J.; Chen, Y.; Wang, Y.; Jiang, T. Selective Ethylene Tetramerization: An Overview. *Inorg. Chem. Front.* **2023**, *10*, 2860–2902.
- (11) Bollmann, A.; Blann, K.; Dixon, J. T.; Hess, F. M.; Killian, E.; Maumela, H.; McGuinness, D. S.; Morgan, D. H.; Neveling, A.; Otto, S.; Overett, M.; Slawin, A. M. Z.; Wasserscheid, P.; Kuhlmann, S. Ethylene Tetramerization: A New Route to Produce 1-Octene in Exceptionally High Selectivities. *J. Am. Chem. Soc.* **2004**, *126*, 14712–14713.
- (12) Overett, M. J.; Blann, K.; Bollmann, A.; Dixon, J. T.; Haasbroek, D.; Killian, E.; Maumela, H.; McGuinness, D. S.; Morgan, D. H. Mechanistic Investigations of the Ethylene Tetramerisation Reaction. *J. Am. Chem. Soc.* **2005**, *127*, 10723–10730.
- (13) Blann, K.; Bollmann, A.; de Bod, H.; Dixon, J. T.; Killian, E.; Nongodlwana, P.; Maumela, M. C.; Maumela, H.; McConnell, A. E.; Morgan, D. H.; Overett, M. J.; Pretorius, M.; Kuhlmann, S.; Wasserscheid, P. Ethylene Tetramerisation: Subtle effects exhibited by N-substituted diphosphinoamine ligands. *J. Catal.* **2007**, *249*, 244–249.
- (14) Killian, E.; Blann, K.; Bollmann, A.; Dixon, J. T.; Kuhlmann, S.; Maumela, M. C.; Maumela, H.; Morgan, D. H.; Nongodlwana, P.; Overett, M. J.; Pretorius, M.; Höfener, K.; Wasserscheid, P. The use of bis(diphenylphosphino)amines with N-aryl functionalities in selective ethylene tri- and tetramerisation. *J. Mol. Catal. A: Chem.* **2007**, *270*, 214–218.
- (15) Kim, S.-K.; Kim, T.-J.; Chung, J.-H.; Hahn, T.-K.; Chae, S.-S.; Lee, H.-S.; Cheong, M.; Kang, S. O. Bimetallic Ethylene Tetramerization Catalysts derived from Chiral DPPDME Ligands: Syntheses, Structural Characterizations, and Catalytic Performance of [(DPPDME)CrCl₃]₂ (DPPDME = S,S- and R,R-chiraphos and meso-achiraphos). *Organometallics* **2010**, *29*, 5805–5811.
- (16) Zhang, J.; Wang, X.; Zhang, X.; Wu, W.; Zhang, G.; Xu, S.; Shi, M. Switchable Ethylene Tri-/Tetramerization with High Activity: Subtle Effect Presented by Backbone-Substituent of Carbon-Bridged Diphosphine Ligands. *ACS Catal.* **2013**, *3*, 2311–2317.
- (17) Alam, F.; Zhang, L.; Wei, W.; Wang, J.; Chen, Y.; Dong, C.; Jiang, T. Catalytic Systems Based on Chromium (III) Silylated-Diphosphinoamines for Selective Ethylene Tri-/Tetramerization. *ACS Catal.* **2018**, *8*, 10836–10845.
- (18) Kim, E. H.; Lee, H. M.; Jeong, M. S.; Ryu, J. Y.; Lee, J.; Lee, B. Y. Methylaluminoxane-Free Chromium Catalytic System for Ethylene Tetramerization. *ACS Omega* **2017**, *2*, 765–773.
- (19) Barman, S.; Jaseer, E. A.; Garcia, N.; Elanany, M.; Khawaji, M.; Xu, W.; Lin, S.; Alasiri, H.; Akhtar, M. N.; Theravalappil, R. A rational approach towards selective ethylene oligomerization via PNP-ligand design with an N-triptycene functionality. *Chem. Commun.* **2022**, *58*, 10044–10047.
- (20) Jiang, T.; Zhang, S.; Jiang, X.; Yang, C.; Niu, B.; Ning, Y. The effect of N-aryl bisphosphineamine ligands on the selective ethylene tetramerization. *J. Mol. Catal. A: Chem.* **2008**, *279*, 90–93.
- (21) Jaseer, E. A.; Garcia, N.; Barman, S.; Khawaji, M.; Xu, W.; Alasiri, H.; Peedikakkal, A. M. P.; Akhtar, M. N.; Theravalappil, R. *ACS Omega* **2022**, *7*, 16333–16340.
- (22) Thompson, M. J.; Borsenberger, V.; Louth, J. C.; Judd, K. E.; Chen, B. Design, Synthesis, and Structure-Activity Relationship of Indole-3-glyoxylamide Libraries Possessing Highly Potent Activity in a Cell Line Model of Prion Disease. *J. Med. Chem.* **2009**, *52*, 7503–7511.
- (23) Esaki, H.; Hattori, T.; Tsubone, A.; Mibayashi, S.; Sakata, T.; Sawama, Y.; Monguchi, Y.; Yasuda, H.; Nosaka, K.; Sajiki, H. Chemoselective Hydrogenation Catalyzed by Pd on Spherical Carbon. *ChemCatChem* **2013**, *5*, 3629–3635.
- (24) Shaikh, Y.; Albahily, K.; Sutcliffe, M.; Fomitcheva, V.; Gambarotta, S.; Korobkov, I.; Duchateau, R. A highly selective ethylene tetramerization catalyst. *Angew. Chem., Int. Ed.* **2012**, *51*, 1366–1369.
- (25) McGuinness, D. S.; Overett, M.; Tooze, R. P.; Blann, K.; Dixon, J. T.; Slawin, A. M. Z. Ethylene Tri- and Tetramerization with Borate Cocatalysts: Effects on Activity, Selectivity, and Catalyst Degradation Pathways. *Organometallics* **2007**, *26*, 1108–1111.
- (26) Boelter, S. D.; Davies, D. R.; Margl, P.; Milbrandt, K. A.; Mort, D.; Vanchura, B. A., II; Wilson, D. R.; Wiltzius, M.; Rosen, M. S.; Klosin, J. Phospholane-Based Ligands for Chromium-Catalyzed Ethylene Tri- and Tetramerization. *Organometallics* **2020**, *39*, 976–987.